Dynamic Modeling of Oil Transport in Vapor Compression Systems

Qiao, Hongtao; Laughman, Christopher R.

Abstract

In this paper, we propose a model describing the dynamics of refrigerant-oil mixture in vapor compression systems. This model uses the approach presented by Thome (1995) to calculate the thermodynamic properties of refrigerant- oil mixture. The governing equations for one-dimensional flow are modified with augmentation of oil mass balance. Partial derivatives of mixture density are carefully computed to ensure the consistence of the choice of state variables for all flow conditions. The existing models for heat exchanger and other components are refined accordingly. Numerical simulation for the start-up operation of an air-conditioning cycle is conducted to evaluate the efficacy of the proposed model. The results for the effect of oil on system performance are provided.

Dynamic Modeling of Oil Transport in Vapor Compression Systems

Hongtao QIAO*, Christopher R. LAUGHMAN

Mitsubishi Electric Research Laboratories,
Cambridge, MA, USA
{qiao, laughman}@merl.com

ABSTRACT

In this paper, we propose a model describing the dynamics of refrigerant-oil mixture in vapor compression systems. This model uses the approach presented by Thome (1995) to calculate the thermodynamic properties of refrigerant-oil mixture. The governing equations for one-dimensional flow are modified with augmentation of oil mass balance. Partial derivatives of mixture density are carefully computed to ensure the consistence of the choice of state variables for all flow conditions. The existing models for heat exchanger and other components are refined accordingly. Numerical simulation for the start-up operation of an air-conditioning cycle is conducted to evaluate the efficacy of the proposed model. The results for the effect of oil on system performance are provided.

Keywords: modeling, heat exchanger, refrigerant-oil mixture, vapor compression, air-conditioning, simulation

1. INTRODUCTION

In vapor compression systems, lubricating oil plays a key role in ensuring an efficient operation of compressors by reducing friction and wear of moving surfaces, providing a seal between high pressure and low pressure sides, and removing heat of compression and helping cooling the internal components. In general, the majority of lubricating oil remains inside the compressor crankcase, while a small portion of oil can be carried out of the compressor by the refrigerant and circulates with it throughout the system.

Lubricating oils typically exist as liquid phase in vapor compression systems as they have a much higher boiling temperature (around 300 °C) than common refrigerants. Consequently, the presence of oil results in changes in the phase behavior and thermophysical properties of refrigerant-oil mixture, which can be treated as a binary zeotropic blend with high temperature glides. Generally, the evaporation process is more susceptible to the presence of oil, since the local boiling point temperature tends to rise relative to the saturation temperature of the pure refrigerant as the evaporation process progresses and the liquid mixture becomes more enriched in oil. In contrast, the effect of oil on the condensation process is less significant because vapor phase is essentially pure refrigerant due to the extremely low vapor pressure of oils comparing to that of refrigerants. Knowledge about the phase behavior of refrigerant-oil mixture is crucial for practitioners in HVAC industries to understand how lubricants affect the operation of HVAC equipment. The vapor-liquid phase equilibrium of refrigerant-oil mixture can be determined by the equation of state (EOS) based on the equality of fugacity for each component in both vapor and liquid phases. However, this approach involves many numerical iterations and is computationally expensive. Therefore, a generalized approach in which empirical equations are used to predict the thermodynamic properties of refrigerant-oil mixture as a function of oil concentration is preferred (Thome 1995) because of its simplicity.

Within the remainder of the system, the lubricant serves as a contaminant and adversely affects the performance of heat exchangers and overall system under most conditions. Numerous experimental studies have been conducted to investigate two-phase heat transfer for refrigerant-oil mixture and the effect of oil was reported to vary nonlinearly with oil mass concentration. For condensation heat transfer, negligible effect of oil was found for low oil mass fractions (below 3%), whereas an unfavorable effect was observed for higher oil mass fractions. However, the presence of oil exhibited mixing effects on evaporation heat transfer, depending on the local operating conditions, i.e., oil enhances heat transfer at low mass velocities and intermediate vapor qualities and induces a very negative effect at high vapor qualities. For the HVAC applications, a large portion of an evaporator often operates in the annular and mist flow regimes with high vapor quality, therefore, overall detrimental effect of oil on evaporation heat transfer was often observed. On the contrary, there is a consensus that lubricant results in a significant increase in two-phase frictional pressure drop compared to oil-free conditions given the fact that oils are much more viscous than refrigerants.

These factors work together, leading to deterioration in the thermal capacity of heat exchangers with increasing oil mass fraction. The adverse effect on the component level is inevitably passed on to the system level, resulting in decline in overall efficiency.

In addition to performance degradation, vapor compression systems also suffer from reliability issues due to the presence of oil, among which flooded start is probably the major one of them. Flooded start occurs when refrigerant migrates from the system and condenses into the compressor oil during off-cycles, due to the vapor pressure of refrigerant being much greater than that of oil. As a result, the sump oil becomes diluted with this condensed liquid. The longer the compressor is idle, the more refrigerant that migrates. When the compressor turns on, the sudden pressure drop in the crankcase will cause the refrigerant in the oil to rapidly flash to vapor. This lead to violent foaming in the crankcase, resulting in very small oil droplets entrained in this vaporization process. The oil level in the crankcase will then drop and mechanical parts will suffer from inadequate lubrication. Flooded start does not only cause loss of oil from the crankcase, it also can cause a form of slugging in the compressor cylinders. With a large eruption of the refrigerant and oil, a relatively large quantity of oil can enter the cylinders. During the compression stroke, damages can occur to the valves, bearings and many other mechanical parts since oil is not compressible.

Furthermore, circulating oil can accumulate in bends and pockets of system components. Consequently, the crankcase in the compressor may suffer from a shortage of oil, resulting in lack-of-lubrication failure. The suction line is often a major location for oil holdup and a minimum refrigerant velocity is required to ensure proper oil return. Oil return becomes more problematic for part-load conditions due to low refrigerant vapor velocities. Therefore, the challenge to the system designer is to ensure that lubricant returns to the compressor satisfactorily under all operating conditions.

It is evident that the design of vapor compression systems not only needs to consider the influence of oil on performance degradation, but also needs to ensure adequate oil return to avoid compressor failure. To achieve this requires a thorough understanding of system characteristics, which are already complex enough under oil-free conditions, let alone the additional dynamics introduced by the oil. While there have been a number of relevant experimental studies available in literature, the most comprehensive results on refrigerant and lubricant distribution during stop-start cycling operation were reported by Peuker (2010). Compared with tedious and expensive experimental investigations, theoretical modeling provides a much more efficient way to explore the effect of oil on system performance, oil transport behavior, oil retention characteristics, and a variety of other associated fluid flow and heat transfer phenomena.

A literature review indicated that there is a dearth of studies on the modeling of oil transport behavior in vapor compression systems. Choi et al. (2009) presented a numerical analysis for oil distribution in commercial air-conditioning systems under steady-state conditions. Zhong et al. (2021) proposed a system model of an automobile air-conditioning system with refrigerant-oil mixture based on the framework of commercial simulation tool GT-SUITE, however, the authors failed to provide modeling details and only the steady-state results regarding the effect of oil on system performance were given. To fill the research gap, this paper intends to develop a detailed model that is capable of capturing the interactions between refrigerant and oil and predicting oil transport behavior in vapor compression cycles. The remainder of the paper is organized as follows. Section 2 provides the modeling details of refrigerant-oil mixture. Section 3 discusses the simulation results. The conclusions are summarized in Section 4.

2. MODELING OF REFRIGERANT-OIL MIXTURE FLOW

The dynamic characteristics of refrigerant-oil mixture flow can be described by the conservation laws that govern a one-dimensional flow with fluid properties varying only in the direction of flow. Consequently, these properties are uniform or averaged at every cross section along the axis of the channel. Additional assumptions used to simplify the models included: (1) refrigerant is miscible with oil, (2) ideal mixing between refrigerant and oil, (3) oil only exists in liquid phase and negligible quantity of oil enters vapor phase, (4) axial heat conduction in the flow direction is ignored, (5) viscous dissipation is neglected, (6) liquid and vapor are in thermodynamic equilibrium in the two-phase region, (7) the potential energy and kinetic energy of the refrigerant are neglected, and (8) dynamic pressure waves are of minor importance and are thus neglected in the momentum equation (Brasz and Koenig, 1983).

The balances of total mass, total energy, and oil mass and total momentum are given as follows.

$$\frac{\partial(\rho A)}{\partial t} + \frac{\partial \dot{m}}{\partial z} = 0 \tag{1}$$

$$\frac{\partial(\rho A h - pA)}{\partial t} + \frac{\partial(\dot{m}\hat{h})}{\partial z} = Pq'' \tag{2}$$

$$\frac{\partial\left[\rho_{mL}(1-\alpha)Aw\right]}{\partial t} + \frac{\partial(\dot{m}c)}{\partial z} = 0 \tag{3}$$

$$A\frac{\partial p}{\partial z} + \tau P = 0 \tag{4}$$

where w is the oil mass fraction in liquid refrigerant-oil mixture, α is the void fraction, ρ is the mean density, ρ_{mL} is the density of liquid refrigerant-oil mixture, c is the oil circulation rate (OCR) defined as the ratio of oil mass flow rate to the total mass flow rate, h is density-weighted specific enthalpy, and $\hat{h}$ is flow-weighed specific enthalpy.

In order to apply the finite volume method to solve the governing equations, the domain of the refrigerant-oil mixture flow needs to be spatially discretized into n control volumes. The staggered grid scheme is used to decouple the equations of continuity and energy with the equation of momentum. There are two types of cells: volume cells (blocks enclosed in black solid lines), and flow cells (blocks enclosed in red dash lines) centered at the interfaces of the volume cells, as shown in Fig. 1. The mass and energy balances are calculated within the volume cell while the momentum balance is calculated between the volume cells, i.e., within the flow cell. Integrating Eqs. (1) - (4) over the ith volume cell yields

$$A\Delta z \frac{d\rho_i}{dt} = \dot{m}_{i-1/2} - \dot{m}_{i+1/2} \tag{5}$$

$$A\Delta z\left(\rho_i \frac{dh_i}{dt} - \frac{dp_i}{dt}\right) = \dot{m}_{i-1/2}\left(\hat{h}_{i-1/2} - h_i\right) - \dot{m}_{i+1/2}\left(\hat{h}_{i+1/2} - h_i\right) + Pq_i''\Delta z \tag{6}$$

$$A\Delta z \frac{d\left[\rho_{mL}(1-\alpha)w\right]}{dt} = \dot{m}_{i-1/2}c_{i-1/2} - \dot{m}_{i+1/2}c_{i+1/2} \tag{7}$$

$$p_i - p_{i+1} = \Delta p_{f,i} \tag{8}$$

It is necessary to introduce additional equations relating the quantities in volume and flow cells.

$$\varphi_{i+1/2} = \varphi_i\delta + (1-\delta)\varphi_{i+1} \tag{9}$$

For convection-dominated flows, the upwind difference scheme is recommended to approximate thermodynamic quantities onto the staggered cells, because the central difference scheme may lead to non-physical solutions (Patankar, 1980).

$$\delta = \begin{cases} 1 \text{ when } \dot{m}_{i+1/2} \geq 0 \\ 0 \text{ when } \dot{m}_{i+1/2} < 0 \end{cases} \tag{10}$$

Therefore, one can easily obtain the flow-weighted enthalpy at the interface of the volume cells (i.e., the center of the flow cells)

$$\hat{h}_{i+1/2} = \begin{cases} \hat{h}_i & \text{when } \dot{m}_{i+1/2} \geq 0 \\ \hat{h}_{i+1} & \text{when } \dot{m}_{i+1/2} < 0 \end{cases} \tag{11}$$

Similarly, oil circulation rate can be related to oil mass fraction.

$$c_{i+1/2} = \begin{cases} (1-\hat{x}_{i+1/2})w_i & \text{when } \dot{m}_{i+1/2} \geq 0 \\ (1-\hat{x}_{i+1/2})w_{i+1} & \text{when } \dot{m}_{i+1/2} < 0 \end{cases} \tag{12}$$

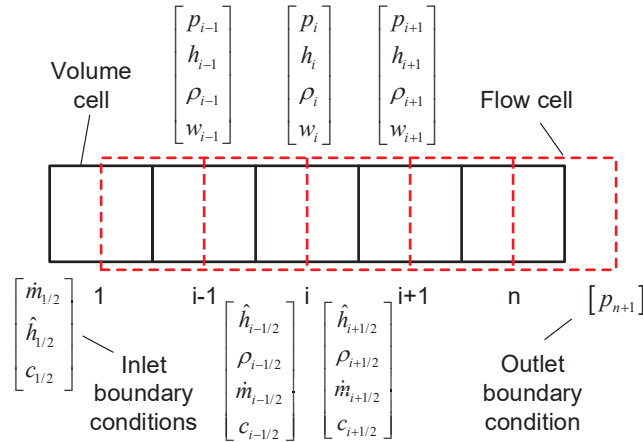where $\hat{x}$ is flow quality that is evaluated with $\hat{h}$.

Fig. 1 Finite volume discretization of refrigerant-lubricant mixture flow

With proper choice of state variables, Eqs. (5) - (8) can be numerically solved if the thermophysical properties of refrigerant-oil mixture, especially the phase equilibrium properties, are readily known. In general, pressure-temperature-concentration of refrigerant-oil mixture can be determined with either the EOS with mixing rules or active coefficient models based on a Gibbs energy formulation. Unfortunately, both methods are iterative in nature and not well suited for the simulation of vapor compression cycles in which the computation time is dominated by the thermophysical property calculations. Therefore, iteration-free empirical equations proposed by Thome (1995) were adopted in our work to calculate the thermodynamic properties of refrigerant-oil mixture, i.e., bubble point temperatures, local oil concentrations, liquid specific heats and enthalpy changes during evaporation. As a result, the additional complexity is modest and there is a minimum impact on the simulation speed.

Fig. 2 illustrated the boiling process of refrigerant-oil mixture. Depending upon the stage of the boiling process, Eq. (5) needs to be handled differently.
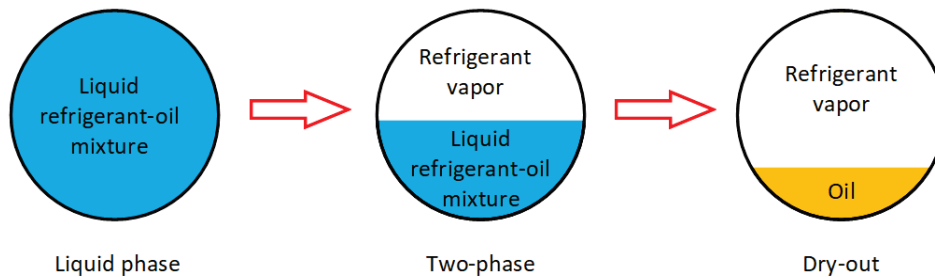

Fig. 2 Illustration of refrigerant-oil mixture boiling

(1) *Liquid phase*

When the temperature is below the bubble point temperature, both refrigerant and oil are in liquid phase and no refrigerant vapor exists. Assuming ideal mixing, the density of refrigerant-oil mixture can be calculated as

$$\rho = \rho_{mL} = \rho_o / \left[1 + (1-w)(\rho_o / \rho_r - 1) \right] \tag{13}$$

where ρ_o is oil density that is a function of temperature only, and ρ_r is refrigerant density evaluated with pressure and temperature. Meanwhile, specific enthalpy of refrigerant-oil mixture is determined by

$$h = (1-w) h_r (p, T) + w h_o (T) \tag{14}$$

It is evident that mixture density is a function of pressure, temperature and oil mass fraction with the following form

$$\rho = \rho (p, T(p, h, w), w) \tag{15}$$

Therefore, we can obtain the partial derivatives of mixture density without providing further details because of space constraint.

$$\left.\frac{\partial \rho}{\partial p}\right|_{h,w} = \left.\frac{\partial \rho}{\partial p}\right|_{T,w} + \left.\frac{\partial \rho}{\partial T}\right|_{p,w} \left.\frac{\partial T}{\partial p}\right|_{h,w} \tag{16}$$

$$\left.\frac{\partial \rho}{\partial h}\right|_{p,w} = \left.\frac{\partial \rho}{\partial T}\right|_{p,w} \left.\frac{\partial T}{\partial h}\right|_{p,w} \tag{17}$$

$$\left.\frac{\partial \rho}{\partial w}\right|_{p,h} = \left.\frac{\partial \rho}{\partial w}\right|_{p,T} + \left.\frac{\partial \rho}{\partial T}\right|_{p,w} \left.\frac{\partial T}{\partial w}\right|_{p,h} \tag{18}$$

Eq. (5) can be rewritten as

$$A\Delta z \left(\left.\frac{\partial \rho_i}{\partial p_i}\right|_{h_i,w_i} \frac{dp_i}{dt} + \left.\frac{\partial \rho_i}{\partial h_i}\right|_{p_i,w_i} \frac{dh_i}{dt} + \left.\frac{\partial \rho_i}{\partial w_i}\right|_{p_i,h_i} \frac{dw_i}{dt} \right) = \dot{m}_{i-1/2} - \dot{m}_{i+1/2} \tag{19}$$

The mass balance of oil can take the following form

$$\rho_i A\Delta z \frac{dw_i}{dt} = \dot{m}_{i-1/2}\left(c_{i-1/2} - w_i\right) - \dot{m}_{i+1/2}\left(c_{i+1/2} - w_i\right) \tag{20}$$

Substituting Eq. (20) into (19) and rearranging gives

$$\left.\frac{\partial \rho_i}{\partial p_i}\right|_{h_i,w_i} \frac{dp_i}{dt} + \left.\frac{\partial \rho_i}{\partial h_i}\right|_{p_i,w_i} \frac{dh_i}{dt} = \frac{\dot{m}_{i-1/2}}{A\Delta z}\left(1 - \left.\frac{\partial \rho_i}{\partial w_i}\right|_{p_i,h_i} \frac{c_{i-1/2} - w_i}{\rho_i}\right) - \frac{\dot{m}_{i+1/2}}{A\Delta z}\left(1 - \left.\frac{\partial \rho_i}{\partial w_i}\right|_{p_i,h_i} \frac{c_{i+1/2} - w_i}{\rho_i}\right) \tag{21}$$

To be consistent, p, h and M_o are selected as the state variables (reasons will be explained later). Consequently, the integral form of the oil mass conservation will be

$$\frac{dM_{o,i}}{dt} = \dot{m}_{i-1/2}c_{i-1/2} - \dot{m}_{i+1/2}c_{i+1/2} \tag{22}$$

Finally, Eqs. (21), (6), (8) and (22) are used to describe the dynamics of refrigerant-oil mixture flow in liquid phase.

It is worthwhile to mention that the presence of oil delays the onset of boiling process since the bubble point temperature of refrigerant-oil mixture is higher than that of pure refrigerant. When the actual temperature is higher than the bubble point temperature of pure refrigerant, but lower than that of refrigerant-oil mixture, refrigerant liquid is in "superheated" state. Under this circumstance, we treat the refrigerant as saturated liquid at the actual temperature to calculate its properties since pressure has negligible effect.

(2) *Two-phase*

When temperature reaches the bubble point temperature, refrigerant starts to vaporize out of the liquid mixture because it is more volatile. Since the vapor pressure of oil is significantly lower than that of refrigerant, it is reasonable to assume that oil concentration in vapor phase is negligible and only refrigerant vapor exists. In this case, liquid refrigerant, liquid oil and vapor refrigerant coexist in a thermodynamic equilibrium.

According to Thome's approach, the bubble point temperature of refrigerant-oil mixture for a given saturation pressure and oil mass fraction can be determined by

$$T_{bub} = a / \left[\ln\left(p\right) - b \right] \tag{23}$$

where both a and b are a polynomial of oil mass fraction.

Based on Eq. (23), the boiling temperature of refrigerant-oil mixture rises with oil mass fraction increasing as the boiling process progresses and can exceed the corresponding saturation temperature of pure refrigerant at the same pressure. As a result, refrigerant in vapor phase is actually superheated even though the mean state of refrigerant-oil mixture is two-phase, then the properties of superheated refrigerant vapor can be easily evaluated with pressure and

temperature using the original EOS of refrigerant. Likewise, refrigerant in the liquid mixture is also superheated, and its properties are calculated as saturated liquid at temperature T_{bub}. Therefore, specific volume of two-phase refrigerant-oil mixture is given by

$$v = v_{mL}(p,T,w) + \frac{h - h_{mL}}{h_{rV}(p,T) - h_{mL}}\left[v_{rV}(p,T) - v_{mL}(p,T,w)\right] \tag{24}$$

where

$$h_{mL} = (1-w)h_{rL}(T) + wh_o(T) = h_{mL}(p,w) \tag{25}$$

h_{mL} is specific enthalpy of liquid refrigerant-oil mixture, h_{rL} is specific enthalpy of liquid refrigerant, and h_{rV} is specific enthalpy of refrigerant vapor. It is easy to know that specific volume v is a function of p, h and w since T is a function of p and w. Therefore, we can calculate the partial derivatives as follows.

$$\left.\frac{\partial v}{\partial p}\right|_{h,w} = \left.\frac{\partial v_{mL}}{\partial p}\right|_{h,w} + \left(v_{rV} - v_{mL}\right)\left.\frac{\partial}{\partial p}\left(\frac{h - h_{mL}}{h_{rV} - h_{mL}}\right)\right|_{h.w} + \frac{h - h_{mL}}{h_{rV} - h_{mL}}\left(\left.\frac{\partial v_{rV}}{\partial p}\right|_{h,w} - \left.\frac{\partial v_{mL}}{\partial p}\right|_{h,w}\right) \tag{26}$$

$$\left.\frac{\partial v}{\partial h}\right|_{p,w} = \left.\frac{\partial v_{mL}}{\partial h}\right|_{p,w} + \left(v_{rV} - v_{mL}\right)\left.\frac{\partial}{\partial h}\left(\frac{h - h_{mL}}{h_{rV} - h_{mL}}\right)\right|_{p.w} + \frac{h - h_{mL}}{h_{rV} - h_{mL}}\left(\left.\frac{\partial v_{rV}}{\partial h}\right|_{p,w} - \left.\frac{\partial v_{mL}}{\partial h}\right|_{p,w}\right) \tag{27}$$

$$\left.\frac{\partial v}{\partial w}\right|_{p,h} = \left.\frac{\partial v_{mL}}{\partial w}\right|_{p,h} + \left(v_{rV} - v_{mL}\right)\left.\frac{\partial}{\partial w}\left(\frac{h - h_{mL}}{h_{rV} - h_{mL}}\right)\right|_{p.h} + \frac{h - h_{mL}}{h_{rV} - h_{mL}}\left(\left.\frac{\partial v_{rV}}{\partial w}\right|_{p,h} - \left.\frac{\partial v_{mL}}{\partial w}\right|_{p,h}\right) \tag{28}$$

With oil mass fraction defined as $w = M_o/[M(1-x)]$, one can deduce its time derivative with some manipulations

$$\frac{dw}{dt} = \frac{\frac{1}{\rho A\Delta z}\left(\frac{\sum \dot{m}}{1-x} - w\sum \dot{m}\right) + \frac{w}{h_{rV} - h}\frac{dh}{dt} - \frac{w}{h_{rV} - h_{mL}}\left(\left.\frac{\partial h_{mL}}{\partial p}\right|_w + \frac{x}{1-x}\left.\frac{\partial h_{rV}}{\partial p}\right|_w\right)\frac{dp}{dt}}{1 + \frac{w}{h_{rV} - h_{mL}}\left.\frac{\partial h_{mL}}{\partial w}\right|_p + \frac{wx}{h_{rV} - h}\left.\frac{\partial h_{rV}}{\partial w}\right|_p} \tag{29}$$

Therefore, Eq. (5) can be reformulated as following with dw/dt given by Eq. (29).

$$A\Delta z\left(\left.\frac{\partial \rho_i}{\partial p_i}\right|_{h_i,w_i}\frac{dp_i}{dt} + \left.\frac{\partial \rho_i}{\partial h_i}\right|_{p_i,w_i}\frac{dh_i}{dt} + \left.\frac{\partial \rho_i}{\partial w_i}\right|_{p_i,h_i}\frac{dw_i}{dt}\right) = \dot{m}_{i-1/2} - \dot{m}_{i+1/2} \tag{30}$$

The remaining governing equations will be the same as in the liquid phase.

(3) *Dry-out*

Substituting $w = 1$ into Eq. (23) gives the dew point temperature of refrigerant-oil mixture. When the temperature reaches the dew point temperature, all the refrigerant has vaporized and there is no more refrigerant dissolved in the oil. In the dry-out condition, oil mass fraction is always unity and the mean density will be a function of static quality instead of oil mass fraction as in the liquid and two-phase conditions.

$$v = (1-x)v_o(T) + xv_{rV}(p,T) \tag{31}$$

where

$$x = \alpha\rho_{rV}/\left[\alpha\rho_{rV} + (1-\alpha)\rho_o\right] \tag{32}$$

$$\alpha = 1 - M_o/\left(A\Delta z\rho_o\right) \tag{33}$$

For the liquid and two-phase conditions, it might be tempting to select p, h and w as the state variables and expand $d\rho/dt$ and dM_o/dt using the chain rule because ρ is a function oil mass fraction. However, it is not the case anymore for the dry-out condition. Therefore, different state variables need to be chosen. To be consistent for all conditions, oil mass M_o instead of oil mass fraction w is selected as a state in addition to p and h.

The partial derivatives of specific volume with respect to p, h and M_o are given by

$$\frac{\partial v}{\partial p}\bigg|_{h,M_o} = (1-x)\frac{\partial v_o}{\partial p}\bigg|_{h,M_o} + x\frac{\partial v_{rV}}{\partial p}\bigg|_{h,M_o} - \left[\frac{v_{rV}-v_o}{h_{rV}-h_o}\frac{\partial h_o}{\partial p}\bigg|_{h,M_o} + \frac{x(v_{rV}-v_o)}{h_{rV}-h_o}\left(\frac{\partial h_{rV}}{\partial p}\bigg|_{h,M_o} - \frac{\partial h_o}{\partial p}\bigg|_{h,M_o}\right)\right] \quad (34)$$

$$\frac{\partial v}{\partial h}\bigg|_{p,M_o} = (1-x)\frac{\partial v_o}{\partial h}\bigg|_{p,M_o} + x\frac{\partial v_{rV}}{\partial h}\bigg|_{p,M_o} + \left[\frac{v_{rV}-v_o}{h_{rV}-h_o}\left(1-\frac{\partial h_o}{\partial h}\bigg|_{p,M_o}\right) - \frac{x(v_{rV}-v_o)}{h_{rV}-h_o}\left(\frac{\partial h_{rV}}{\partial h}\bigg|_{p,M_o} - \frac{\partial h_o}{\partial h}\bigg|_{p,M_o}\right)\right] \quad (35)$$

$$\frac{\partial v}{\partial M_o}\bigg|_{p,h} = (1-x)\frac{\partial v_o}{\partial M_o}\bigg|_{p,h} + x\frac{\partial v_{rV}}{\partial M_o}\bigg|_{p,h} - \left[\frac{v_{rV}-v_o}{h_{rV}-h_o}\frac{\partial h_o}{\partial M_o}\bigg|_{p,h} + \frac{x(v_{rV}-v_o)}{h_{rV}-h_o}\left(\frac{\partial h_{rV}}{\partial M_o}\bigg|_{p,h} - \frac{\partial h_o}{\partial M_o}\bigg|_{p,h}\right)\right] \quad (36)$$

Accordingly, Eq. (5) can be reformulated as

$$\frac{\partial \rho_i}{\partial p_i}\bigg|_{h_i,M_{o,i}}\frac{dp_i}{dt} + \frac{\partial \rho_i}{\partial h_i}\bigg|_{p_i,M_{o,i}}\frac{dh_i}{dt} = \dot{m}_{i-1/2}\left(\frac{1}{A\Delta z} - \frac{\partial \rho}{\partial M_{o,i}}\bigg|_{p_i,h_i}\right) - \dot{m}_{i+1/2}\left(\frac{1}{A\Delta z} - \frac{\partial \rho}{\partial M_{o,i}}\bigg|_{p_i,h_i}\right)c_{i+1/2} \quad (37)$$

Once again, the remaining governing equations will be the same as in the previous cases.

It should be pointed out that all above equations are also applicable to the condensation process with a caveat that the calculation of dew point temperature will not be affected by the presence of oil since only refrigerant exists in vapor phase.

3. RESULTS AND DISCUSSIONS

An air source air-conditioning cycle was constructed to model the oil transport behavior during start-up operation. The air-conditioning system used R32 as the working fluid, and consisted of a condenser, an evaporator, a compressor and an electronic expansion valve, as shown in Fig. 3. The compressor was a low-side rotary compressor, and both heat exchangers were louvered fin-and-tube heat exchangers. A feedback loop closed on the suction superheat with a setpoint of 10 K, driving the opening of the LEV. The evaporator was operated with inlet air temperature at 27 °C, whereas the ambient environment was 35 °C. The start-up simulation was intended to emulate the scenarior of the system being shut off for a long period of time. Therefore, the entire system was initialized at an equlibrium pressure of 17.7 bar, with superheated refrigerant vapor in the condenser and two-phase refrigerant in the evaporator. The total amount of the lubricant was 5.5 oz. All the oil was in the compressor crankcase before the start-up operation.
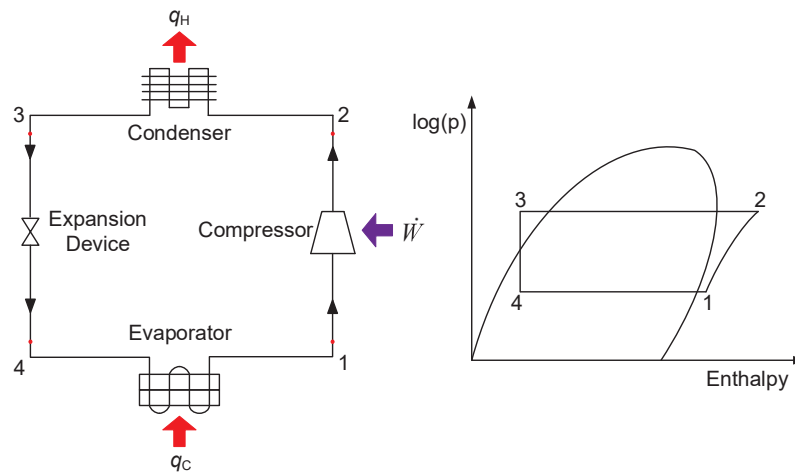

Fig. 3 A four-component vapor compression system

The dynamics of refrigerant-oil mixture flow were modeled using the method described in the previous section. The modeling techniques of the airside and tube walls were given in Qiao et al. (2015), and the details of other component models can be found in Qiao et al. (2017). These models were augmented by a set of empirical closure relations

describing the single- and two-phase heat transfer coefficients and frictional pressure drops for the refrigerant-oil mixture flow, as listed in Table 1. The Levy void fraction model (Levy, 1967) was used to compute the two-phase refrigerant-oil mixture mass inventory. A tube-by-tube approach was employed for the heat exchanger analysis, i.e., the performance of each tube was analyzed separately and each tube was associated with different refrigerant and air parameters. These models were implemented in the Modelica language using the Dymola 2020x simulation environment (AB Dassault Systemes, 2020), and run on a laptop with an Intel i7 processor with 32 Gb of RAM; the DASSL solver was used to integrate the set of differential algebraic equations with a tolerance of 10^{-5}.

Table 1 Heat transfer and pressure drop correlations

Conditions	Correlation
Single-phase heat transfer	Dittus & Bolter (1985)
Condensation heat transfer	Dobson & Chato (1998)
Evaporation heat transfer	Gungor & Winterton (1986)
Single-phase pressure drop	Blasius (Incropera & DeWitt, 1996)
Condensation pressure drop	Lockhart & Martinelli (1949)
Evaporation pressure drop	Jung et al. (1989)

The start-up simulation lasted for 1000 seconds and the pertinent outputs were given in Fig. 4. The pressure transients were shown in Fig. 4a. The discharge pressure increased rapidly within the first 30 seconds, then decreased for about one minute, and thereafter gradually recovered the ascending trend and finally leveled off. The surge in the discharge pressure was attributed to the imbalance between the mass flow entering and leaving the condenser, and to the delayed condensation of the refrigerant. The subsequent decrease was a result of insufficient replenishment of refrigerant from the compressor due to enlarged pressure ratios. The suction pressure declined at the very beginning and increased afterwards. The decrease in the suction pressure was caused by the depletion of refrigerant from the evaporator.

It was evident from Fig. 4b that evaporator superheat was stabilized at the target, i.e., 10 K, after 600 seconds. This superheat was called "apparent superheat", which was defined as the difference between the actual temperature and the corresponding dew point temperature of pure refrigerant at the exit pressrue. However, the flow quality leaving the evaporator was still well below unity, indicating an incomplete vaporization. The contradiction can be explained by the elevated boiling temperature due to the presence of oil. Refrigerant-oil mixture acted as a zeotropic blend with a large temperature glide, and its local bubble point temperature increased signficantly as oil became richer in liquid phase in the ending tubes of evaporator. Therefore, refrigerant could leave the evaporator with much higher temperature, but still in wet conditions.

Fig. 4c and 4d illustrated the transients of oil circulation rate at different locations of both heat exchangers. Oil carry-out through the compressor depended on the amount of oil in the compressor crankcase. When the compressor was powered on, the oil level was full, resulting in the highest oil circulation rate entering the condenser. After oil escaped into the system, the oil level declined gradually, lowering the oil circulation rate out of the compressor. Eventually, oil circulation rate in the system stablized around 2.8%.

Oil retention in system components was shown in Fig. 4e. It can be observed that the majority of oil was holded up by the compressor, followed by the condenser and then evaporator. These resutls were straightforward since oil tended to accumulate in the components with prolonged liquid region. More rigorously, pipes, especially suction line, and accumulator should be included in the analysis because they were the most critical components with highest values of oil retention per unit length. However, this is beyond the scope of the current work and will not be discussed in this paper.

The transients of airside head loads and compressor power were given in Fig. 4f. The airside heat load of condenser and evaporator increased rapidly within the first three minutes, and then gradually approached the steady-state value of around 6 kW and 5 kW, respectively. The compressor power exhibited similar trends and finally plateaued at 1 kW.

4. CONCLUSIONS

This work presented a new model to describe the dynamics of refrigerant-oil mixture in vapor compression systems. Numerical analysis was conducted to explore the effect of oil on system performance of an air-conditioning cycle. It was found that the presence of oil led to incomplete evaporation even with large superheat leaving the evaporator. Meanwhile, simulation results indicated that oil tended to accumulate more in the condenser than the evaporator. Future work includes the modeling of oil retention in the suction line and accumulator, and development of a more rigorous compressor model to capture the underlying physics of flooded start so that a comprehensive investigation on refrigerant-oil behavior under various modes of operation can be performed.
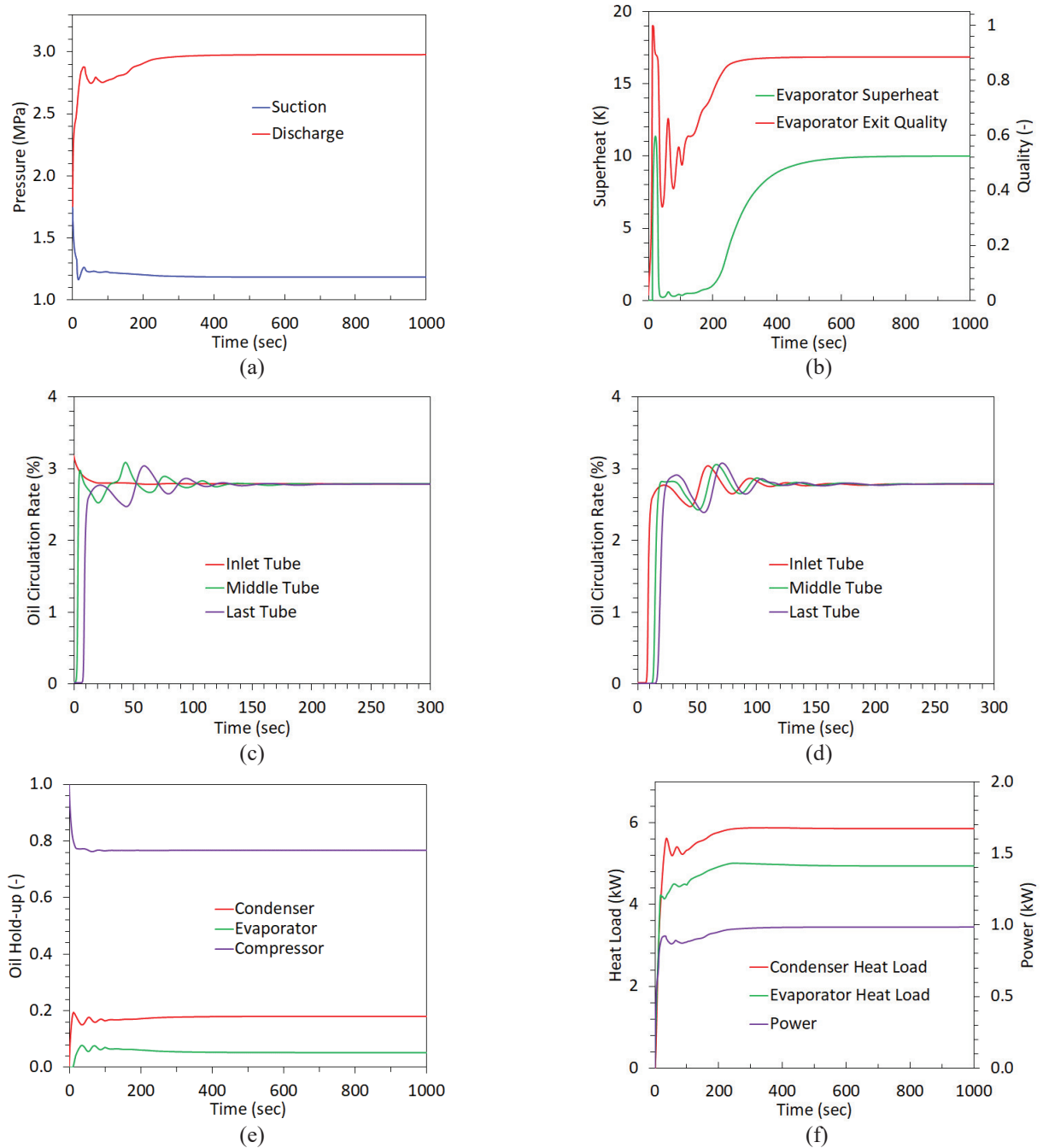

Fig. 4 Start-up simulation results: (a) pressure transients; (b) evaporator superheat and exit quality; (c) OCRs of condenser; (d) OCRs of evaporator; (e) oil mass distribution; (f) heat loads and power

NOMENCLATURE

Symbols

A	cross sectional area		x	quality
c	oil circulation rate		α	void fraction
h	specific enthalpy		ρ	density
M	mass		τ	wall shear stress
$\dot{m}$	mass flow rate			
P	perimeter		*Subscripts*	
p	pressure		bub	bubble point
q''	heat flux		mL	liquid mixture
T	temperature		o	oil
t	time		r	refrigerant
w	oil mass fraction		rV	refrigerant vapor
v	specific volume			

REFERENCES

AB Dassault Systemes. Dymola 2020.

Brasz J.J. and Koenig, K., 1983. Numerical methods for the transient behavior of two-phase flow heat transfer in evaporators and condensers. Numerical Properties and Methodologies in Heat Transfer, ed. T.M. Shih, Springer Verlag, Berlin, 461-476.

Choi, J.W. et al., 2009. A numerical study on oil retention and migration characteristics in the heat pump system. *J. Mech. Sci. Technol*. 23, 1858-1865.

Dittus, F.W., and Boelter, L.M.K., 1985. Heat transfer in automobile radiators of the tubular type. *Int. Commun. Heat Mass* 12 (1), 3-22.

Dobson, M. K., and Chato, J. C., 1998. Condensation in smooth horizontal tubes. *ASME J. Heat Transfer* 120, 193-213.

Gungor, K.E., Winterton, R.H.S., 1986. A general correlation for flow boiling in tubes and annuli. *Int. J. Heat Mass Transfer* 29 (3), 351–358.

Incropera, F.P. and DeWitt, D.P., 1996. Introduction to heat transfer (3rd Ed.). John Wiley & Sons, New York.

Jung, D. S., McLinden, M., Radermacher, R., Didion, D., 1989. A study of flow boiling heat transfer with refrigerant mixtures. *Int. J. Heat Mass Transfer* 32 (9), 1751-1764.

Levy, S., 1967. Forced convection subcooled boiling prediction of vapor volumetric fraction. *Int. J. Heat Mass Transfer* 10, 951–965.

Lockhart, R.W. and Martinelli, R.C., 1949. Proposed correlation of data for isothermal two-phase, two-component flow in pipes. Chem. Eng. Prog. S. Ser. 45, 39-48.

Patankar, S.V., 1980. Numerical heat transfer and fluid flow. New York: Hemisphere Publishing Corporation, Taylor and Francis Group.

Peuker, S., 2010. Experimental and analytical investigation of refrigerant and lubricant migration. Ph.D. Thesis, University of Illinois at Urbana-Champaign.

Qiao, H., Aute, V., Radermacher, R., 2015. Transient modeling of a flash tank vapor injection heat pump system - Part I: Model development. *Int. J. Refrigeration* 49, 169-182.

Qiao, H., Laughman, C.R., Burns, D., Bortoff, S., 2017. Dynamic characteristics of an R410-A multi-split variable refrigerant flow air-conditioning system. 12th IEA Heat Pump Conference, Rotterdam, Netherlands.

Thome, J.R., 1995. Comprehensive thermodynamic approach to modeling refrigerant-Lubricating oil mixtures. *HVAC&R Res*. 1, 110-125.

Thome, J.R., 2004. Chapter 16: Effects of oil on thermal performance of heat exchangers. *Engineering Data Book III* (16-1). Wolverine Tube, Inc.

Zhong, Y., Tiwari, A., Jain, A., Spasov, M., 2021. A model of heat exchangers and automotive AC system with refrigerant-oil mixtures. 17th International Refrigeration and Air Conditioning Conference of Purdue, West Lafayette, IN, USA.